Surface-initiated graft polymerization on multiwalled carbon nanotubes pretreated by corona discharge at atmospheric pressure

Lihua Xu,[a] Zhengping Fang,[ab] Ping'an Song[a] and Mao Peng[*a]

Surface-initiated graft polymerization on multi-walled carbon nanotubes pretreated with a corona discharge at atmospheric pressure was explored. The mechanism of the corona-discharge-induced graft polymerization is discussed. The results indicate that MWCNTs were encapsulated by poly(glycidyl methacrylate) (PGMA), demonstrating the formation of PGMA-grafted MWCNTs (PGMA-g-MWCNTs), with a grafting ratio of about 22 wt%. The solubility of PGMA-g-MWCNTs in ethanol was dramatically improved compared to pristine MWCNTs, which could contribute to fabricating high-performance polymer/MWCNTs nanocomposites in the future. Compared with most plasma processes, which operate at low pressures, corona discharge has the merit of working at atmospheric pressure.

Since Iijima's landmark paper in 1991,[1] carbon nanotubes (CNTs) have attracted great attention because of their extraordinary properties and potential applications in various fields including field-emission devices,[2,3] gas storage media,[4] nanoelectronic devices[5,6] and polymeric composites.[7–12] However, these applications have been limited by a number of crucial problems, such as the agglomeration and poor dispersion of CNTs in polymer matrices because of the strong intrinsic van der Waals forces of CNTs. Therefore, a variety of strategies have been employed to modify CNTs to improve their solubility or suspending ability in organic solvents and compatibility with polymer matrices, especially with polar polymers.[13–20]

Among the strategies above, plasma treatment of CNTs is of great importance because it is non-polluting, time-saving and has been demonstrated to generate successfully hydroxyl, carbonyl, carboxyl, amine and fluorine groups on the surface of CNTs.[20–25] Moreover, the plasma-induced graft polymerization of vinyl monomers has been found to be an extremely attractive method of chemical modification of CNTs.[26,27] Unfortunately, these plasma treatment methods are generally executed at pressures below one atmosphere, which restricts their continuous operation and their scaling-up to industrial levels. In contrast, corona discharge can be carried out in air, nitrogen and argon atmospheres at room temperature and works well at normal atmospheric pressure. Previously, numerous studies have investigated the possibility of corona discharge for the surface modification of polymeric materials.[28,29] The results show that corona discharge is an effective method for introducing active sites to polymer surfaces which can subsequently initiate free-radical grafting reactions, so that robust polymer brushes can be covalently immobilized on the surface of substrates. At the same time, corona discharge has also been successfully employed to introduce polar groups to the surface of carbon fibers and improve their interface interactions with polymer matrices.[30,31] Considering the convenience and effectiveness of corona discharge, we expect that corona discharge is also suitable for the surface modification of CNTs and the following graft polymerization to prepare polymer-grafted CNTs. There is no similar report in the literature to our knowledge.

In our study, multi-walled carbon nanotubes (MWCNTs) were first treated with a N_2 plasma created by corona discharge at normal atmospheric pressure, and then transferred to glycidyl methacrylate (GMA) to perform the graft polymerization. The polymer was successfully grafted onto MWCNTs and the suspending ability of the modified MWCNTs in ethanol was greatly improved.

MWCNTs (prepared by chemical vapor deposition) with a length in the range of 10–20 μm and an outer diameter varying from 30 to 50 nm were purchased from Chengdu Organic Chemicals Co., Ltd., Chinese Academy of Sciences and were used as received. GMA with a purity of 95% and 1,1-diphenyl-2-picryhydrazyl (DPPH) were purchased from Sigma-Aldrich. Other chemicals were analytical grade and used as received.

A home-made corona discharge apparatus (Fig. 1) was used for pre-treating the MWCNTs. Two flat aluminium electrodes of 25 cm × 25 cm were fixed in parallel with an air gap of 1.5 cm between them in a sealed container. The bottom electrode was covered with a silicone rubber plate of 5.0 mm in thickness as a barrier, on which a layer of MWCNTs was dispersed and treated with the corona discharge.

Prior to the plasma reaction, high purity N_2 at 1 atmospheric pressure was introduced into the container at a flow rate of 1.5 L min^{-1}. The corona discharge power was 300 W at 19.8 kHz and MWCNTs were exposed to the corona discharge for a certain time.
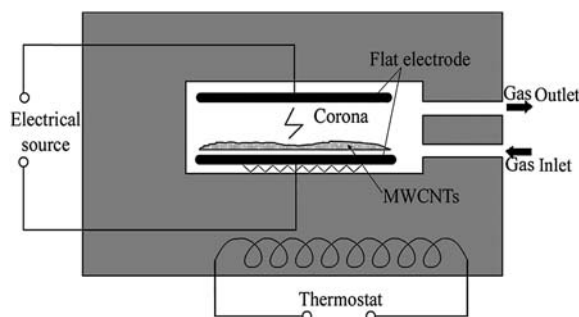
[a]Institute of Polymer Composites, Zhejiang University, Key Laboratory of Macromolecular Synthesis and Functionalization, Ministry of Education, Hangzhou 310027, China. E-mail: pengmao@zju.edu.cn; Fax: +86 571 87953712
[b]Lab of Polymer Materials and Engineering, Ningbo Institute of Technology, Zhejiang University, Ningbo 315100, China

Fig. 1 Schematic diagram of the corona discharge apparatus.

After that, the treated MWCNTs were transferred into GMA that had been purged by nitrogen. The graft polymerization was allowed to occur for 4 h under ultrasonication at 70 °C. After the graft polymerization, the product poly(glycidyl methacrylate)-grafted MWCNTs (PGMA-*g*-MWCNTs) were purified by vacuum filtration and then rinsed with acetone under ultrasonication. The PGMA-*g*-MWCNTs were rinsed three times to remove any unreacted monomer, oligomer or homopolymers of GMA which were generated during thermal polymerization. The purified PGMA-*g*-MWCNTs were finally dried at 80 °C under vacuum for 12 h.

The number of active sites formed on the surface of MWCNTs was determined by a DPPH method,[32,33] in which MWCNTs treated by corona discharge and pristine MWCNTs were immersed in a 1.0×10^{-4} M benzene solution of DPPH and heated to 70 °C for 24 h. The amount of DPPH consumed by the decomposed peroxide on the surface of MWCNTs was determined by the difference of absorbance at 520 nm in the ultraviolet–visible spectra (UV2550 Shimadzu, Japan) of the treated MWCNTs and pristine MWCNTs.

X-Ray photoelectron spectroscopy (XPS) was carried out on a Thermo VG Scientific ESCALAB 250 spectrometer (UK). Transmission electron microscopy (TEM) images were collected by using a JEM 1230 TEM (JEOL, JP) operated at 120 kV. Thermogravimetric analysis (TGA) was performed on an SDT Q600 thermal analyzer (TA instrument, USA) at a heating rate of 10 °C min^{-1} in nitrogen. Field-emission scanning electron microscopy (FE-SEM) images were recorded on a SIRION-100 FE-SEM (FEI, The Netherlands) at an accelerating voltage of 10 kV. The chemical structure of PGMA-*g*-MWCNTs was characterized by Fourier-transform infrared (FTIR) using KBr pellets on a Vector-22 FTIR spectrometer (Bruker, Germany).

It is widely accepted that plasma processes are rather complex and a good understanding of the interactions between plasmas and substrate surfaces is difficult,[34] However, many previous studies have shown that radicals can be generated on the surface of polymers[35,36] or CNTs[21–23] after plasma treatments. Most of the radicals will develop into peroxide and hydroperoxides with the participation of oxygen in the plasma or the exposure of air after plasma treatment in inert gases such as argon and nitrogen. The peroxides formed are stable at room temperature for a long time. The thermal decomposition of the peroxides can initiate the polymerization of many monomers including acrylic acid and acrylamide, as well as result in crosslinking of polymer coatings. In this study, the DPPH method is used to determine whether there are active sites on the surface of MWCNTs after the corona-discharge treatment. The results show that the concentration of the active sites including free radicals and peroxides on the surface of the MWCNTs is 1.15×10^{-7} mol mg^{-1}. Since these can initiate free-radical polymerization, a suggested
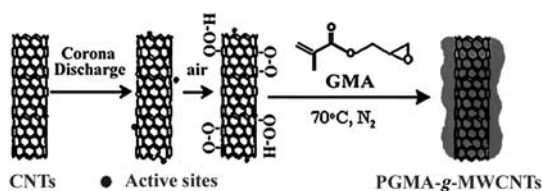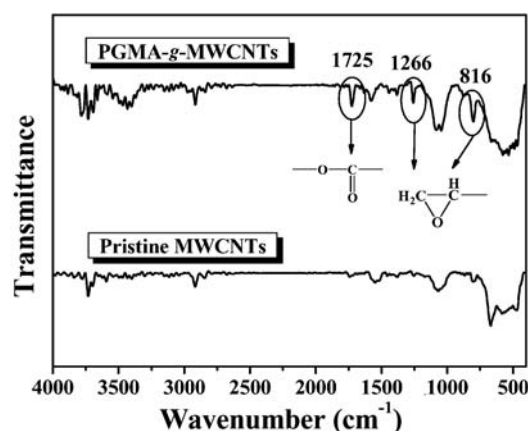

Fig. 3 FTIR spectra of the pristine MWCNTs and the PGMA-*g*-MWCNTs.

mechanism for the corona-discharge-induced graft polymerization on the surface of MWCNTs is presented in Fig. 2.

The FTIR spectrum of PGMA-*g*-MWCNTs in Fig. 3 shows that after the graft polymerization of GMA, there is a much stronger peak at 1725 cm^{-1}, which corresponds to the carbonyl groups of the PGMA. Moreover, the absorption band at 1266 cm^{-1} can be ascribed to the asymmetrical stretching of C–O–C and the peak at 816 cm^{-1} is due to the bone vibrations of the epoxy groups. By comparing with the FTIR spectrum of the pristine MWCNTs, it can be concluded that the PGMA is successfully grafted onto the surface of the MWCNTs by the corona-discharge-induced surface modification.

Fig. 4 shows the XPS survey spectra (A), O1s (B) and C1s core-level spectra of the pristine MWCNTs, the MWCNTs treated by corona discharge and then exposed to air for oxidization (denoted as O-MWCNTs) and the PGMA-*g*-MWCNTs. The time of corona-discharge treatment was 20 s for O-MWCNTs and PGMA-*g*-MWCNTs. The pristine MWCNTs show a strong C1s peak at the binding energy of around 284.6 eV, and a very weak peak at around 532.8 eV assigned to O1s. For O-MWCNTs, the relative intensity of the O1s peak at around 532.5 eV is stronger, indicating that the amount of oxygen on the surface of MWCNTs increases after the corona-discharge treatment, in good agreement with the result of the DPPH method. As for the PGMA-*g*-MWCNTs, the O1s peak at 532.8 eV becomes much stronger, suggesting an effective grafting of PGMA onto the surface of MWCNTs. Furthermore, detailed information of the O1s core-level spectra is shown in Fig. 4(B). Compared with pristine MWCNTs, O-MWCNTs have a new peak at 330.8 eV, which can be ascribed to peroxides according to previous studies.[37–39] The peak around 531.7 eV belongs to the ester carbonyl group of the PGMA, which approves the successful modification of the MWCNTs by corona-discharge-induced graf polymerization. Similarly, the C1s spectra in Fig. 4(C) indicate that after the corona-discharge treatment, the C1s peak at 286.5 eV for C–O increases, and after graft polymerization the C1s peaks at 286.3 eV for C–O and 287.3 eV for C=O and at 289.0 for COO species are also strengthened,[40] The result indicates that PGMA is grafted onto the surface of MWCNTs, in good agreement with the FTIR results.

The carbon and oxygen atomic concentrations as well as the C/O ratios were calculated according to the XPS data, as summarized in Table 1. It was found that after the corona-discharge treatment and graft polymerization, the atomic carbon concentration decreases
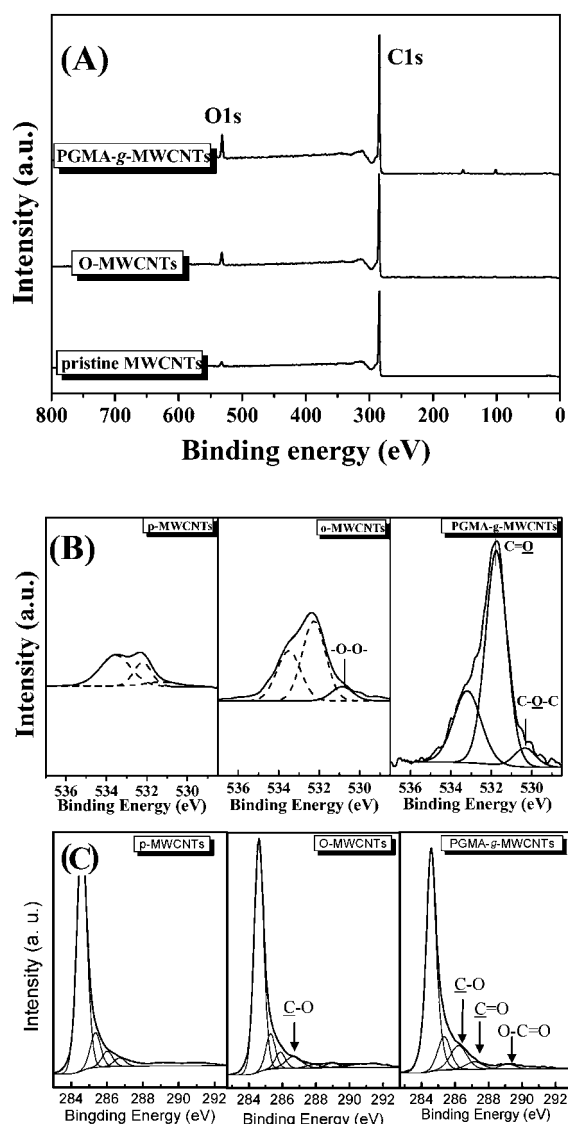

Fig. 2 A suggested mechanism for the corona-discharge-induced graft polymerization.

Fig. 4 (A) XPS survey spectra, (B) O1s spectra, and (C) C1s core-level spectra of pristine MWCNTs, O-MWCNTs and PGMA-*g*-MWCNTs.

Table 1 The element concentrations and C/O ratios of pristine MWCNTs, O-MWCNTs and PGMA-*g*-MWCNTs

Sample	Elemental concentration (at%)		
	C	O	C/O ratio
Pristine CNTs	97.49	2.51	38.8
O-MWCNTs	92.78	7.22	12.9
PGMA-*g*-MWCNTs	90.66	9.34	9.70

while simultaneously the oxygen concentration increases. Considering the molecular weight of GMA, the amount of PGMA grafted onto the surface of MWCNTs can be calculated to be about 27 wt%.

As shown in Fig. 5(A), in nitrogen, the thermal decomposition (pyrolysis) of pristine MWCNTs (sample 1) is quite limited and the weight retention is about 98.7 wt% at 600 °C. O-MWCNTs (sample 2) exhibit a larger weight loss, and the corresponding derivative thermograms (DTG) in Fig. 5(B) show a small decomposition peak
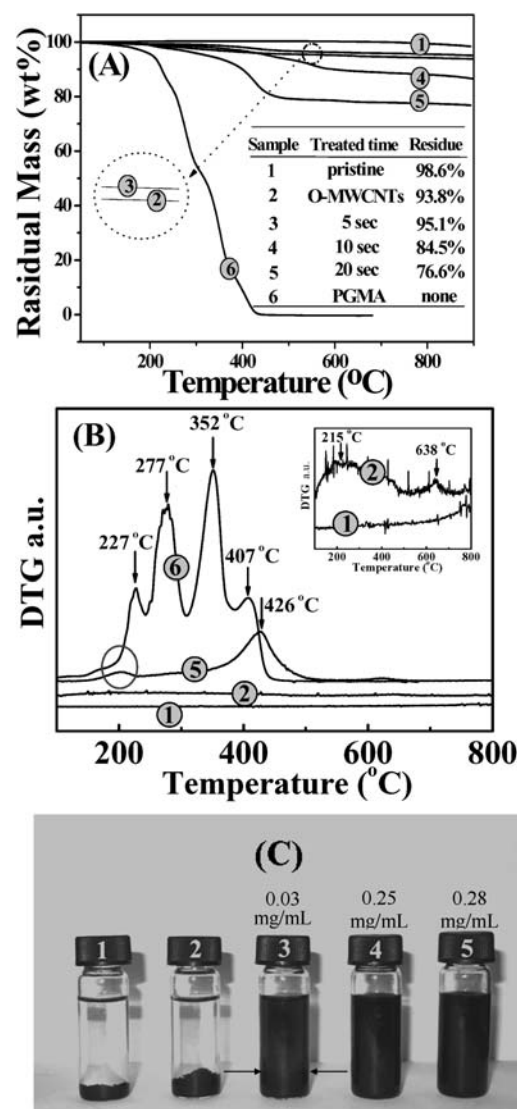

Fig. 5 (A) TGA curves of (1) pristine MWCNTs, (2) O-MWCNTs, PGMA-*g*-MWCNTs with corona-discharge treatment time of (3) 5 s, (4) 10 s and (5) 20 s, and (6) neat PGMA; (B) corresponding derivative thermogravimetric (DTG) curves; (C) digital image of various MWCNTs dispersed in ethanol. The numbers are the solubilities of the samples.

at around 215 °C which does not exist in the thermogram of pristine MWCNTs. This indicates that after corona discharge, some functional groups that can be thermally decomposed are attached to the surface of the MWCNTs. This is highly consistent with the results of the XPS analysis and DPPH method. TGA was also conducted for the PGMA-*g*-MWCNTs with corona-discharge treatment times of 5, 10 and 20 s for samples 3, 4 and 5, respectively, as shown in Fig. 5(A). For a corona-discharge treatment of 5 s (sample 3), few active sites could be induced onto the MWCNTs, and the weight loss of the PGMA-*g*-MWCNTs was close to that of the O-MWNCTs, indicating the failure of graft polymerization. However, with the increase in treatment time, the weight retention at 450 °C decreases which is attributed to the increased grafting ratio with the increase in time of the corona-discharge treatment. This indicates that the concentration of active sites on the surface of MWCNTs can be increased to some extend by increasing the corona-discharge treatment time. However,
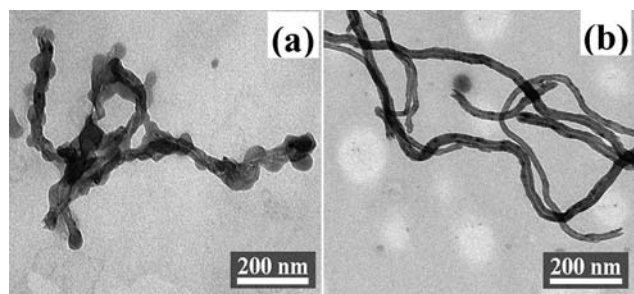
Fig. 6 TEM images of (a) PGMA-*g*-MWCNTs, and (b) pristine MWCNTs.

it was found that the grafting ratio of PGMA on MWCNTs did not always increase with the increase in treatment time, for example when the treatment time was further prolonged to 120 s, the grafting ratio was similar to that when the treatment was 20 s. The DTG curve of PGMA-*g*-MWCNTs (sample 5) indicates that the peak temperature of thermal degradation mainly occurs at about 426 °C, a higher value than that of the pure PGMA. This demonstrates the enhanced thermal stability of PGMA immobilized on the surface of MWCNTs because of certain interactions between MWCNTs and PGMA. Furthermore, because PGMA grafted on MWCNTs decomposes almost completely at temperatures above 600 °C, the grafting ratio of PGMA can be calculated on the basis of the residual weights at 600 °C of pristine MWCNTs, PGMA-*g*-MWCNTs and neat PGMA, which is about 22 wt% for sample 5, in satisfactory agreement with the value obtained from XPS (27 wt%).

Fig. 5(C) shows a digital image of various MWCNT samples dispersed in ethanol after being left for a week in ambient conditions. Both the pristine MWCNTs and the O-MWCNTs precipitate completely at the bottom of the vial while the PGMA-*g*-MWCNTs with processing time of 5 s appearing as partial precipitation, as revealed by the arrows. The solubility is about 0.03 mg mL^{-1}. The PGMA-*g*-MWCNTs with 10 and 20 s treatment exhibit a dramatically improved ability to suspend in ethanol. The suspensions are visually black without precipitation and have solubilities of 0.25 and 0.28 mg mL^{-1}, respectively. It is expected that the improved solubility in ethanol of MWCNTs make it possible that the dispersion of PGMA-*g*-MWCNTs in some polar polymers can also be improved. This will be investigated in the future.

The TEM image of PGMA-*g*-MWCNTs [Fig. 6(a)] reveals that in contrast to pristine MWCNTs [Fig. 6(b)], the PGMA-*g*-MWCNTs are encapsulated by polymer shells with a heterogeneous thickness, indicating that the creation of active sites on MWCNTs during the corona-discharge treatment is not uniform. But it is indicative that the modification of MWCNTs and the following graft polymerization of GMA on MWCNTs were successful.

Fig. 7 shows SEM images of pristine MWCNTs and PGMA-*g*-MWCNTs. Apparently, pristine MWCNTs are smooth, with a diameter of about 30–50 nm, while PGMA-g-MWCNTs are encapsulated by thick shells, increasing the diameter of PGMA-*g*-MWCNTs to 60–120 nm. Consistent with the TEM observations, the PGMA-*g*-MWCNTs are not uniform in diameter. As indicated by the arrows in Fig. 7(d), some sections of the PGMA-*g*-MWCNTs are thick with a diameter of about 120 nm, while the neighboring sections have thinner diameters of about 40–60 nm, revealing that the graft polymerization on the surface of MWCNTs is not uniform. The in-homogeneity can be contributed to either the different reactivity of
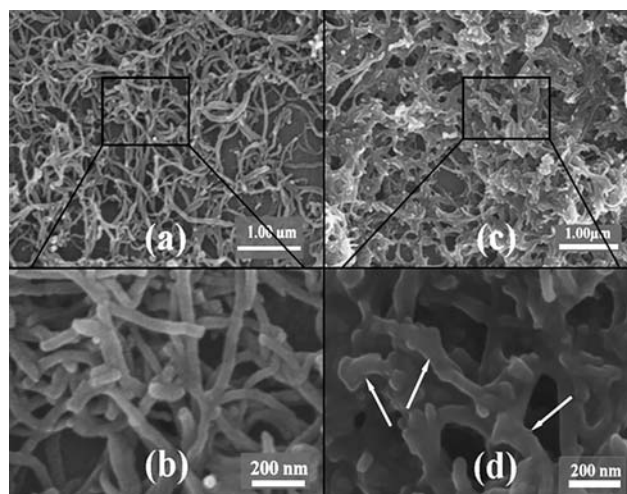

Fig. 7 SEM images of pristine MWCNTs (a, b) and PGMA-*g*-MWCNTs (c, d).

different positions on the surfaces of CNTs or the in-homogeneity of the plasma. To explain the in-homogeneities formed in thin films prepared by corona-discharge-assisted chemical vapor deposition, Thyen *et al.*[41] assumed that local electrical irregularities on the substrate surface might lead to in-homogeneities of the electric field in these areas. The in-homogeneities would be initially established when an initial micro-discharge deposited electrical charges on the substrate surface, causing the next micro-discharge to prefer the previous location where the electrical charges are located and deposit more electrical charges. According to this mechanism, it is believed that the active sites generated by corona-discharge treatment are distributed non-uniformly on the surface of the MWCNTs, consequently, more PGMA deposits on the active sites on the MWCNTs and becomes polymerized, resulting in the non-uniform morphology of PGMA-*g*-MWCNTs.

Corona-induced graft polymerization was used for the surface modification of CNTs for the first time. The results demonstrate that MWCNTs treated by corona discharge at atmospheric pressure can successfully initiate the graft polymerization of GMA onto the surface of MWCNTs and PGMA is covalently bonded to the surface of MWCNTs at a grafting ratio of about 22 wt%. A core–shell structure formed after the graft polymerization and the polymer shells on the surface of MWCNTs were not uniform. The suspending ability of the PGMA-*g*-MWCNTs in ethanol is much better than that of pristine MWCNTs and O-MWCNTs. Comparing with previously reported methods for grafting polymers onto CNTs, this method has some merits, such as the rapid corona-discharge treatment at atmospheric pressure and the relatively high grafting ratio. It is expected that the PGMA-*g*-MWCNTs could be applied as reinforcing fillers for polymer/MWCNT composites in the future.

Acknowledgements

References

1 S. Iijima, *Nature*, 1991, **354**, 56.
2 T. Feng, J. H. Zhang, Q. Li, X. Wang, K. Yu and S. C. Zou, *Phys. E.*, 2007, **36**, 28.
3 C. J. Lee, J. Park, S. Y. Kang and J. H. Lee, *Chem. Phys. Lett.*, 2000, **326**, 175.
4 S. C. Mu, H. L. Tang, S. H. Qian, M. Pan and R. Z. Yuan, *Carbon*, 2006, **44**, 762.
5 J. Zhao, Q. Y. Gao, C. Gu and Y. Yang, *Chem. Phys. Lett.*, 2002, **358**, 77.
6 R. H. Baughman, A. A. Zakhidov and W. A. de Heer, *Science*, 2002, **297**, 787.
7 S. Wang, R. Liang, B. Wang and C. Zhang, *Chem. Phys. Lett.*, 2008, **457**, 371.
8 X. H. Chen, J. F. Wang, M. Lin, W. B. Zhong, T. Feng, X. H. Chen and *et al.*, *Mater. Sci. Eng., A*, 2008, **492**, 236.
9 S. Campidelli, C. Klumpp, A. Bianco, D. M. Guldi and M. Prato, *J. Phys. Org. Chem.*, 2006, **19**, 531.
10 S. Jiang, J. Deng and W. Yang, *Macromol. Rapid Commun.*, 2008, **29**, 1521.
11 H. J. Park, J. Kim, J. Y. Chang and P. Theato, *Langmuir*, 2008, **24**, 10467.
12 P. A. Song, L. H. Xu, Z. H. Guo, Y. Zhang and Z. P. Fang, *J. Mater. Chem.*, 2008, **18**, 5083.
13 W. Z. Yuan, Y. Mao, H. Zhao, J. Z. Sun, H. P. Xu, J. K. Jin and et al, *Macromolecules*, 2008, **41**, 701.
14 J. G. Wang, Z. P. Fang, A. J. Gu, L. H. Xu and F. Liu, *J. Appl. Polym. Sci.*, 2006, **100**, 97.
15 L. Zhang, V. U. Kiny, H. Q. Peng, J. Zhu, R. F. M. Lobo, J. L. Margrave and et al, *Chem. Mater.*, 2004, **16**, 2055.
16 P. Petrov, X. Lou, C. Pagnoulle, C. Jérôme, C. Calberg and R. Jérôme, *Macromol. Rapid Commun.*, 2004, **25**, 987.
17 S. Bhandari, M. Deepa, A. K. Srivastava, C. Lal and R. Kant, *Macromol. Rapid Commun.*, 2008, **29**, 1959.
18 J. A. Kim, D. G. Seong, T. J. Kang and J. R. Youn, *Carbon*, 2006, **44**, 1898.
19 C. Gao, H. K. He, L. Zhou, X. Zheng and Y. Zhang, *Chem. Mater.*, 2009, **21**, 360.
20 C. Gao, C. D. Vo, Y. Z. Jin, W. W. Li and S. P. Armes, *Macromolecules*, 2005, **38**, 8634.
21 L. Valentini, J. Macan, I. Armentano, F. Mengoni and J. M. Kenny, *Carbon*, 2006, **44**, 2196.
22 U. Vohrer, N. P. Zschoerper, Y. Koehne, S. Langowski and C. Oehr, *Plasma Processes Polym.*, 2007, **4**, S871.
23 L. Valentini, D. Puglia, I. Armentano and J. M. Kenny, *Chem. Phys. Lett.*, 2005, **403**, 385.
24 T. Xu, J. H. Yang, J. W. Liu and Q. Fu, *Appl. Phys. A: Mater. Sci. Process.*, 2008, **90**, 431.
25 R. Ionescu *et al.*, *Sens. Actuators, B*, 2006, **113**, 36.
26 C. H. Tseng, C. C. Wang and C. Y. Chen, *Chem. Mater.*, 2007, **19**, 308.
27 C. H. Tseng, C. C. Wang and C. Y. Chen, *Nanotechnology*, 2006, **17**, 5602.
28 J. X. Lei and X. Liao, *Eur. Polym. J.*, 2001, **37**, 771.
29 S. J. Park and J. S. Jin, *J. Colloid Interface Sci.*, 2001, **236**, 155.
30 E. Desimoni, A. M. Salvi, F. Langerame and J. F. Watts, *J. Electron Spectrosc. Relat. Phenom.*, 1997, **85**, 179.
31 E. Desimoni, A. M. Salvi, U. B. Ceipidor and I. G. Casella, *J. Electron Spectrosc. Relat. Phenom.*, 1994, **70**, 1.
32 M. Suzuki, A. Kishida, H. Iwata and K. Ikada, *Macromolecules*, 1986, **19**, 1804.
33 C. Wang and J. R. Chen, *Appl. Surf. Sci.*, 2007, **253**, 4599.
34 W. T. Ford, in *Chemically Modified Surfaces*, ed. H. A. Mottola and J. R. Steinmetz, Elsevier Science B.V. 1992, pp. 155.
35 S. Turmanova, M. Minchev, K. Vassilev and G. Danev, *J. Polym. Res.*, 2008, **15**, 309.
36 F. Seto, Y. Muraoka, N. Sakamoto, A. Kishida and M. Akashi, *Angew. Makromol. Chem.*, 1999, **266**, 56.
37 J. X. Wu, M. S. Ma, X. M. Liu, J. S. Zhu, M. R. Ji, P. S. Xu and T. X. Zhao, *Phys. Rev. B: Condens. Matter*, 1995, **51**, 14286–14292.
38 K. C. C. Kharas and J. H. Lunsford, *J. Am. Chem. Soc.*, 1989, **111**, 2336.
39 K. Otsuka, T. Ando, S. Suprapto, Y. Wang, K. Ebitani and I. Yamanaka, *Catal. Today*, 1995, **24**, 315.
40 X. P. Zou, E. T. Kang, K. G. Neoh, Y. Zhang, K. L. Tan, C. Q. Cui and T. B. Lim, *Polym. Adv. Technol.*, 2001, **12**, 583.
41 R. Thyen, A. Weber and C. P. Klages, *Surf. Coat. Technol.*, 1997, **97**, 426.